



Estimation of atmospheric particle formation rates through an analytical formula: Validation and application in Hyytiälä and Puijo, Finland

Elham Baranizadeh¹, Tuomo Nieminen¹, Taina Yli-Juuti¹, Markku Kulmala², Tuukka Petäjä², Ari
5 Leskinen^{1,3}, Mika Komppula³, Ari Laaksonen^{1,4}, Kari E. J. Lehtinen^{1,3}

¹Department of Applied Physics, University of Eastern Finland, Kuopio, Finland

²Department of Physics, University of Helsinki, Finland

³Finnish Meteorological Institute, Kuopio, Finland

⁴Climate research Unit, Finnish Meteorological Institute, Helsinki, Finland

10 *Correspondence to:* Elham Baranizadeh (elham.baranizadeh@uef.fi)

Abstract. The formation rates of 3-nm particles were estimated at SMEAR IV, Puijo (Finland) where the continuous measurements extend only down to 7 nm in diameter. We extrapolated the formation rates at 7 nm (J_7) down to 3 nm (J_3) based on an approximate solution to the aerosol general dynamic equation, assuming a constant condensational growth rate, a power-law size dependent scavenging rate and negligible self-coagulation rate for the nucleation mode particles. To
15 evaluate our method, we first applied it to new-particle formation (NPF) events in Hyytiälä (Finland), which extend down to 3 nm, and, therefore, J_3 and J_7 can be determined directly from the measured size distribution evolution. The Hyytiälä results show that the estimated daily mean J_3 slightly overestimate the observed mean J_3 , but a promising 84% of the estimated J_3 are within a factor of 2 from the measured ones. However, when considering detailed daily time evolution, the agreement is typically poor presumably due to uncertainties in estimated growth rates which are required in order to calculate the time-lag
20 between formation of 3-nm and 7-nm particles. At Puijo, the mean and median J_7 for clear NPF days during April 2007-December 2015 were 0.23 and 0.07 cm⁻³s⁻¹, respectively, while the extrapolated mean and median J_3 were 0.47 and 0.13 cm⁻³s⁻¹, respectively.

1 Introduction

Atmospheric new particle formation (NPF) events, i.e. nucleation and subsequent growth of newly formed particles have
25 received increasing attention due to their impact on climate and human health (Kulmala et al., 2004; Merikanto et al., 2009; Nie et al., 2014, Kerminen et al., 2012; Fuzzi et al., 2015, Minguillón et al., 2015 and references therein). Many studies have been conducted to find out which variables cause and which possibly inhibit NPF events. Sulfuric acid, water and ammonia



30 have already long been considered important molecules for atmospheric new particle formation (Weber et al., 1995; Weber et al., 1996; Korhonen et al., 1999; Kulmala et al., 2000; Laaksonen et al., 2008; Xiao et al., 2015). More recently, studies show that amines, ions, and oxidation products of volatile organic compounds can play an important role in NPF events either by participating in the nucleation itself or by stabilizing the nucleated clusters (e.g. Almeida et al., 2013; Berndt et al., 2014; Kirkby et al., 2016). However, several features at the nucleation level including the actual mechanism and other possible vapors involved (Kulmala et al., 2006; Lehtinen et al., 2007) remain unknown.

35 The lack of exact knowledge of NPF mechanisms is partly because at several locations particle size distribution measurements do not extend to nucleation size range but instead start at ca. 3 nm or even at larger sizes (e.g. 7 or 10 nm). This limits the use of the particle data in NPF studies and poses a challenge in understanding NPF globally. In addition, the actual nucleation rates of critical clusters sizes (sub-2-nm in diameter) remain unknown. Even with data obtained by the new
40 condensation particle counters (CPC), that have cut-off mobility diameters of sub-2 nm (Sgro and Fernández de la Mora, 2004; Iida et al., 2009; Vanhanen et al., 2011; Kuang et al., 2012; Wimmer et al., 2013), the determination of nucleation rates still involves approximation.

Measuring sub-3-nm particles is a challenging task because of their diffusion loss during transporting the sample, difficulties in collecting representative samples for electrical detection, difficulties in charging them for electrical size-selection
45 (classification), their insufficient amount to be chemically analyzed, and the need for a very high supersaturation condition to grow them to large enough sizes that they can be optically detected (Kulmala et al., 2012). Because of these challenges in measuring small particles, methods to extrapolate size distributions and formation rates below the measurement range have been suggested by McMurry and Friedlander (1979), McMurry (1982; 1983), Weber et al. (1996); Kerminen and Kulmala (2002); Kerminen et al. (2003); Lehtinen et al. (2007) and most recently by Kürten et al. (2015). We are, however, not aware
50 of another study in which these methods have been tested with atmospheric measurement data.

Our study has two main goals. Firstly, we aim to estimate 3 nm particle formation rates J_3 for Puijo, where continuous size distribution measurements have been going on since 2006. We estimate the J_3 by a scaling method based on aerosol dynamics theory for the range 3 - 7 nm, because the measured size range at Puijo has been only down to 7 nm in diameter.
55 Therefore, our second main goal is to validate our method to estimate J_3 . For this, we use size distributions measured at Hyytiälä, where detailed particle size distribution measurements down to 3 nm have been performed since 1996. From the Hyytiälä data we can thus evaluate formation rates both at 3 nm and 7 nm. The fraction of particles that survives the scavenging by larger aerosols is determined by the ratio of their growth and scavenging rates (Kerminen et al., 2004b). In this study, we use the method of Lehtinen et al. (2007) in which time and size independent particle growth rate and, time
60 independent but size dependent coagulation sink are assumed.



2 Methods

2.1 Data sets and site descriptions

In this study we use the aerosol size distribution measurements at two different SMEAR (Station for Measuring Ecosystem-Atmosphere Relations) stations in Finland: SMEAR II located in Hyytiälä and SMEAR IV in Kuopio. SMEAR II (Hyytiälä, southern Finland; 61°51' N, 24°17' E, 181 m a.s.l.) is characterized by boreal coniferous forest. The main pollution sources are the city of Tampere (60 km away) and the buildings at the station. These sources are most effective when the wind is from the southwest direction (Kulmala et al., 2001). For this study we analyzed aerosol size distributions measured at SMEAR II with a Differential Mobility Particle Sizer (DMPS; Aalto et al., 2001), with a cut-off size at 3 nm, between years 2000-2012.

70

At SMEAR IV the instruments are set up at the top of the Puijo observation tower (62°54'34" N, 27°39'19" E), 306 m and 224 m above the sea level and the surrounding lake level, respectively). Puijo tower is located in the city of Kuopio (Eastern Finland), a semi-urban environment with surroundings characterized by forest with conifer and deciduous (mostly birch) trees, and many lakes. The main local sources surrounding the tower are a paper mill (direction 35°, distance >1.4 km), the city center (direction 120-155°, distance 1.6-3.2 km), a heating plant (direction 160°, distance 3.5 km), a highway and residential areas (see Leskinen et al. (2009) and Portin et al. (2014) for more details). The aerosol size distribution is measured with a twin-DMPS (Winklmayr et al., 1991; Jokinen and Mäkelä, 1997) covering the size range 7-800 nm (Leskinen et al., 2009). The twin-DMPS consists of two differential mobility analyzer (DMA) tubes, one shorter with 11-cm length and another one longer with 28-cm length, and a condensation particle counter (TSI Model 3010 CPC) after each DMA tube. In both DMPS systems, the sample is neutralized (before it enters to the DMA) into charge equilibrium by a beta radiation source (Ni-63 10 mCi=370 MBq). The size range measured by the longer tube is 27-800 nm with 29 discrete bins and 7-49 nm with 17 discrete bins for the shorter tube. The full particle size distribution (7-800 nm) is measured every 12 minutes (Leskinen et al., 2009). At Puijo there is a twin-inlet system for aerosol-cloud interaction studies: one inlet removes cloud droplets (when the station is in a cloud) and collects only the interstitial particles and the other inlet collects the total aerosol, i.e. cloud droplets and interstitial particles. When the station is not in a cloud, the size distribution measured from both inlets are the same. In this study, we used the data from the total aerosol inlet and analyzed aerosol size distributions measured between April 2007 and December 2015.

85

2.2 Data analysis method

Kerminen and Kulmala (2002) derived an analytical formula which links the “real” particle formation rate and the “apparent” formation rates of particles of larger sizes for which measurements are available (typically above 3 nm). The formula was later improved by Lehtinen et al. (2007) by (1) correcting the slightly inaccurate size dependence of the

90



coagulation sink, and (2) removing the unnecessary assumption of the identity of the condensing vapor. According to the formula (equation (7) in Lehtinen et al., 2007) one can estimate the formation rate of smaller particles (J_{d_1}) with diameter d_1 , for which no measurements are available, from formation rate of measured larger particles (J_{d_2}) with diameter d_2 , as follows:

$$J_{d_1} = J_{d_2} \cdot \exp\left(\gamma \cdot d_1 \cdot \frac{CoagS(d_1)}{GR}\right), \quad (1)$$

$$\text{with } \gamma = \frac{1}{m+1} \left(\left(\frac{d_2}{d_1}\right)^{m+1} - 1 \right) \text{ and } m = \frac{\log[CoagS(d_2)/CoagS(d_1)]}{\log[d_2/d_1]},$$

where $CoagS$ is the coagulation sink of smaller particles (diameter d_1) onto the background particles, and GR is the particle growth rate (which is assumed to be constant from diameter d_1 to diameter d_2).

In this study, we apply the Eq. (1) to estimate the apparent formation rates of particles of 3 nm in diameter at Puijo where the size distribution of particles below 7 nm is not measured. To derive Eq. (1) (i.e. equation (7) in Lehtinen et al., 2007), it was assumed that the growth rate between d_1 and d_2 is constant. This assumption, however can fail especially for sizes below 3 nm, where some recent studies have indicated strong size dependence of GR (Kuang et al., 2012; Kulmala et al., 2013).

Korhonen et al. (2014) modified Eq. (1) to also include either linear or power-law type size dependent growth rate and tested the method by using modelled NPF events. In their studies especially the method assuming power-law type growth rate gave promising results with various types of size dependent growth profiles. However, in this study, we assume a constant GR because as mentioned earlier a strong size-dependency of GR has been reported for very small particles typically below 3 nm (e.g. Kuang et al., 2012) rather than for larger sizes. The other assumption when deriving Eq. (1) is that the nucleating particles are lost only by coagulation onto larger pre-existing particles.

To evaluate Eq. (1) against measurements, we use the particle size distribution evolution data during nucleation event days from SMEAR II. There the measurements have extended down to 3 nm in diameter, and therefore, one is able to get apparent formation rates at 7 nm (J_7) and at 3 nm (J_3) directly from measurements. We then set $d_1 = 3$ nm and $d_2 = 7$ nm in Eq. (1) and calculate $J_{3,obs}$ and $J_{7,obs}$ as outlined in Kulmala et al. (2012) and slightly improved in Vuollekoski et al. (2012). Here we use the subscript *obs* to indicate *observed* apparent formation rates J . The formation rate of particles of 3 nm ($J_{3,obs}$) and 7 nm ($J_{7,obs}$) in diameter from measured aerosol size distribution were calculated as follows:

$$J_{3,obs} = \frac{dN_{3-7}}{dt} + n_7 \cdot GR_{7-20} + N_{3-7} \cdot CoagS(d_{GMD}), \quad (2)$$



where $n_7 = \frac{N_{5-9}}{9-5}$ and $d_{GMD} = \sqrt{3 \times 7}$ nm.

125

$$J_{7,obs} = \frac{dN_{7-10}}{dt} + n_{10} \cdot GR_{7-20} + N_{7-10} \cdot CoagS(d_{GMD}), \quad (3)$$

where $n_{10} = \frac{N_{8-12}}{12-8}$ and $d_{GMD} = \sqrt{7 \times 10}$ nm.

130 Here N_{3-7} , N_{5-9} , N_{7-10} and N_{8-12} are the number concentration of particles within size ranges 3-7 nm, 5-9 nm, 7-10 nm and 8-12 nm, respectively, and n_7 and n_{10} are the size distribution function at 3 nm and 7 nm, respectively. The coagulation sink (*CoagS*) terms were calculated directly from the measured particle size distributions, taking into account the hygroscopicity effects using the parametrization of Laakso et al. (2004) who used the hygroscopic growth factor parametrization by Zhou (2001). We used a parabolic differentiation method to the measured number concentration to obtain its time-derivative (the
135 first term in Eq. (2) and Eq. (3)). The method fits a second order polynomial to seven data points centered at the data point where derivative is calculated while at the edges a parabola is fit through the first or last six data points, from which the derivative is calculated directly. Also, to avoid spurious fluctuations in the second and third terms in equations 2 and 3, the N_{3-7} , N_{5-9} , N_{7-10} and N_{8-12} were smoothed using a moving average (over five data points) filter.

140 The estimated formation rate J_3 was then calculated based on Eq. (1):

$$J_{3,est}(t) = J_{7,obs}(t') \cdot \exp\left(\gamma(t) \cdot 3nm \cdot \frac{CoagS(d_1=3nm)}{GR_{3-10}}\right), \quad (4)$$

Note $J_{3,est}$ at time t is calculated based on $J_{7,obs}$ at time t' , where $t = t' - \frac{4nm}{GR_{3-10}}$, thus accounting for the growth time of the
145 3 nm particles to 7 nm particles. To average over this time interval needed for growth, the m and $CoagS(d_1)$ values are calculated as medians of the corresponding values during time t to t' .

To determine the growth rates required in this study, we first used the automated algorithm developed by Hussein et al. (2005) for fitting log-normal modes to the measured size distributions. The algorithm assumes that the size distribution is a
150 superposition of 1-3 log-normal modes and at each measurement time optimizes three unknown parameters for each mode to fit the measurements. The parameters for each individual log-normal mode are the mode number concentration N_i , geometric variance σ_g^2 , and geometric mean diameter D_{pg} . We then estimate GR by fitting the geometric mean diameter D_{pg} of the growing nucleation mode as a function of time; the slope of the fitted line determines the GR in the desired particle size ranges. We also determined the standard error (*SE*) of the GR estimates when fitting D_{pg} values respect to time to obtain GR .
155 We left out the days where the growth rates required in the aforementioned equations (i.e. GR_{3-10} and/or GR_{7-20}) were not



quantifiable. We chose the size range 3-10 nm rather than 3-7 nm to determine the GR in the exponential term of equation 4 (denoted as GR_{3-10}). This was done to increase the number of data points in the GR fitting and thereby to improve the reliability of the fitted GR .

160 After evaluating the analysis method with SMEAR II data, we applied the method for Puijo where the DMPS detection range extended only down to 7 nm. To estimate the formation rate of 3-nm particles at Puijo we adapted Eq. (4) by replacing GR_{3-10} with GR_{7-20} due to lack of DMPS measurements below 7 nm. However, as it will be shown in section 3.1, using GR_{7-20} instead of GR_{3-10} does not affect the accuracy of estimated J_3 for NPF events in Hyytiälä, which is an indication that the size dependence of the growth rate in the range 3-20 nm is typically weak. The $J_{7,obs}$ was calculated with the same
 165 method as was used for Hyytiälä (i.e. using equation 3).

3 Results and discussion

3.1 Analysis of estimated J_3 in Hyytiälä (Finland)

Figure 1 shows the comparison of estimated formation rates $J_{3,est}$ (Eq. (4)) with the observed ones $J_{3,obs}$, as calculated directly from the measured size distribution evolution according to Eq. (2) in Hyytiälä. We analyzed 65 NPF event days for
 170 which the formation and growth rates could be quantified. Each data point in Figure 1-a represents the arithmetic mean of the 3-nm particle formation rates ($J_{3,est}$ and $J_{3,obs}$) for a single NPF day during the time window from 07:00 to 19:00 local time. The results show that the estimated mean $J_{3,est}$ values agree reasonably well with $J_{3,obs}$ with correlation coefficient 0.78 and 85 % of estimated $J_{3,est}$ are within the factor of two of the observed $J_{3,obs}$. Equation (4) seems to have a tendency of overestimating the formation rate of 3-nm particles. We calculated the arithmetic mean of all data points (the total mean)
 175 presented in Figure 1-a. The total means of $J_{3,obs}$, $J_{3,est}$ and $J_{7,obs}$ (not shown in the figure) are 0.21, 0.27 and 0.14 # cm⁻³ s⁻¹, respectively, confirming the tendency of Eq. (4) in overestimating the 3-nm particle formation rates. The color code of Figure 1-a indicates the ratio of the relative standard error (SE) of GR_{3-10} and GR_{3-10} (i.e. SE/GR_{3-10}). According to Figure 1-a no relationship between uncertainty in GR estimates and formation rate estimates is seen. For example the data points close to the 1:1 line consist of both days with high and days with low values for SE/GR_{3-10} .

180

Moreover, we also compared the estimated and observed J_3 values using daytime median values (not shown here), resulting in a correlation coefficient of 0.73 between $J_{3,obs}$ and $J_{3,est}$. The median $J_{3,est}$ values are, however, even more overestimated than the corresponding mean values and only 38% of estimated $J_{3,est}$ are within a factor of two of the observed $J_{3,obs}$. Total medians (median of daily-median values) of $J_{3,obs}$, $J_{3,est}$ and $J_{7,obs}$ are 0.05, 0.106 and 0.047 # cm⁻³ s⁻¹.

185



In addition, we replaced GR_{3-10} with GR_{7-20} in Eq. (4) as will be needed to estimate $J_{3,est}$ in Puijo. Results show that although the correlation coefficient improves to 0.93, a smaller fraction (78%) of $J_{3,est}$ data points are within the factor of two of $J_{3,obs}$ values, and subject to more bias (overestimation). However, these changes are minor and do not significantly affect the results. The total mean of $J_{3,est}$ changed from 0.27 to 0.31 # cm⁻³ s⁻¹ after replacing GR_{3-10} with GR_{7-20} in Eq. (4).

190

Furthermore, we also tested how replacing GR_{3-10} with GR_{3-7} in Eq. (4) affected the estimated $J_{3,est}$ values. Replacing GR_{3-10} with GR_{3-7} resulted in similar bias (i.e. towards overestimation) and agreement between $J_{3,est}$ and $J_{3,obs}$ mean values, to what was obtained from replacing GR_{3-10} with GR_{7-20} : the correlation coefficient slightly improved (0.82) with slightly less $J_{3,est}$ data points (80%) within the factor of two of $J_{3,obs}$. In general replacing GR_{3-10} with GR_{3-7} did not affect the results (i.e. agreement level between of $J_{3,est}$ and $J_{3,obs}$) by much.

195

Figure 1-b shows $J_{3,obs}$ versus $J_{3,est}$ values with the same 10-minute temporal resolution as for the measured size distribution. The points are within the time window from 07:00 to 19:00 local time. With this higher temporal resolution $J_{3,obs}$ and $J_{3,est}$ are not correlated (correlation coefficient = 0.17) despite that their daily mean values presented in Figure 1-a correlate clearly; only 32% of the estimated $J_{3,est}$ are within factor of two of the observed $J_{3,obs}$. The main reason for this is the lack of success in estimating the time lag between the formation of 3-nm and 7-nm particles (see for example the Figure 3-b presented later in this section), which then results in an incorrect time shift for the time evolution of J_3 , even though the daily average values agree reasonably well.

200

After replacing GR_{3-10} with GR_{7-20} in Eq. (4), still 31% of estimated 10-minute $J_{3,est}$ are within factor of two of the observed $J_{3,obs}$, correlation coefficient slightly worsens to 0.13 and, the $J_{3,est}$ data are subject to more bias (positive bias thus overestimation). We, therefore, conclude that replacing GR_{3-10} with GR_{7-20} both for mean $J_{3,est}$ values and 10-minute values, has only a minor effect on the results thus using GR_{7-20} to estimate J_3 values in Puijo is reasonable.

205

Figure 2 shows examples of the time evolution of the particle size distribution as well as the different formation rates J on three NPF days in Hyytiälä. For some NPF days, the estimated time-dependence (or time-lag between 3-nm and 7-nm particle formation rates) and values of $J_{3,est}$ are in fairly-good agreement with those of observed $J_{3,obs}$ (see e.g. Figure 2-d). However, the time-dependency of $J_{3,est}$ is not consistent with $J_{3,obs}$ for most of the days and, instead, typically the $J_{3,est}$ peak occurs earlier than the $J_{3,obs}$ peak (see e.g. Figure 2-e), indicating that our method of estimating GR is not satisfactory and typically underestimates the GR values. In order to investigate how well Eq. (4) estimates the time evolution of the 3-nm particles we visually chose the days during which a clear peak in each of the $J_{7,obs}$, $J_{3,obs}$ and $J_{3,est}$ time evolution curves could be observed (39 days out of 65 days). For these events, we extracted the time difference between 3-nm and 7-nm particle formation from 1) the observed time between peaks in $J_{3,obs}$ and $J_{7,obs}$ (named here observed time-lag), and 2) from

215



growth time $t' - t = 4 \text{ nm}/GR_{3-10}$ (named estimated time-lag) which is also equal to the time difference between $J_{3,est}$ and
 220 $J_{7,obs}$. Figure 2-f shows an example of a NPF day for which the $J_{3,est}$ and $J_{3,obs}$ are dramatically different. This is due to the
 burst in the number concentration which appeared mostly within the size range 3-7 nm (chosen to calculate $J_{3,obs}$) and is thus
 not included in the size range 7-10 nm from which $J_{7,obs}$ is calculated and then scaled to $J_{3,est}$. Therefore, Eq. 4 can give
 quite inaccurate results for NPF days associated with e.g. this type of inhomogeneity in the particle number concentrations in
 different size ranges. It can be also concluded that visual inspection of the data is still valuable - cases like this are very
 225 challenging for automatic data analysis routines. Figure 3 shows the estimated time-lag versus the observed time-lag. As can
 be seen from the figure, the estimated time-lag is mostly longer (toward earlier times of $J_{3,obs}$) than the observed time-lag.
 There are 15 NPF days for which the estimated time-lag is within 1.5 hours of the observed time-lag. Overall these results
 from analyzing Hyytiälä data show that Eq. (4) can be used to estimate the mean formation rates of 3-nm particles with
 reasonably good accuracy. However, the performance in predicting detailed time-evolution of the 3-nm particle formation
 230 rate is poor in most NPF days with the methods that we use for GR estimation.

3.2 Estimation of J_3 in Puijo (Finland)

For the aerosol size distribution data in Puijo, the NPF event days were first recognized visually and classified as
 “quantifiable” and “non-quantifiable” based on whether or not the event is homogeneous enough to allow quantification of
 the basic characteristics such as formation and growth rates (Dal Maso et al., 2005). Therefore, our data pool consists of
 235 event (E), non-event (NE) and undefined days, the last being days during which the evolution of the size distribution is too
 unclear for definitive determination of whether or not NPF has been occurring. We noticed that there are two types of
 undefined days in Puijo. One is characterized with a burst in the number concentration of particles of the smallest detectable
 sizes but doesn't seem to show the characteristics of a NPF event day (i.e. growth to larger sizes, see e.g. Figure 4-a) and
 most likely originate from local emissions. In the other type, some particles appear in larger sizes (with minor growth),
 240 which may or may not be originated from NPF processes. (e.g Figure 4-b) like the first type. Note that 48 and 44% of the
 days are missing during years 2010 and 2012, respectively. The monthly number and yearly fraction of NPF event days
 recorded in Puijo from year 2007 to 2015 are shown in Figure 5. The figure shows that a maximum number of event days
 occurred during spring time similar to NPF events reported in Hyytiälä (Dal Maso et al., 2005). It is also worth noting that
 the fraction of event days is monotonically increasing from 2012 to 2015. There are 75 quantifiable NPF event days for
 245 which we calculated the $J_{3,est}$ at Puijo. Figure 6 shows the seasonal medians of $J_{3,est}$ and $J_{7,obs}$, GR_{7-20} and coagulation sink
 for 7-nm particles ($CoagS(d=7 \text{ nm})$) for the quantifiable NPF event days in Puijo. The total mean and median of $J_{3,est}$ are
 0.47 and 0.13, respectively, while the corresponding values for $J_{7,obs}$ are 0.23 and 0.07 $\#cm^{-3}s^{-1}$, respectively. Total means of
 GR_{7-20} and $CoagS$ of 7-nm particles for NPF days are 2.34 nm/h and 1.5×10^{-4} 1/s, respectively. Thus, the mean GR at Puijo
 is somewhat lower compared to Hyytiälä where mean value of $GR = 4.3$ nm/h is reported for period April 2003- December
 250 2009 (Yli-Juuti et al., 2011).



Table 1 summarizes the seasonal means of parameters presented in Figure 6. The seasonal mean 3-nm particle formation rates seem to have the highest values during spring ($0.52 \text{ #cm}^{-3} \text{ s}^{-1}$ for 50 NPF days) and summer ($0.53 \text{ #cm}^{-3} \text{ s}^{-1}$ for 12 NPF days) and drops significantly in fall. The seasonal median of the growth rate has its maximum in summer (4.14 nm/h) and minimum in spring (2.30 nm/h). The seasonal median *CoagS* values, however, seem to be rather constant in Puijo in contrast to Hyttiälä.

4 Conclusions

In this study, the formation rates of 3-nm particles in SMEAR IV, Puijo (Finland) were estimated. The measurements at Puijo extend only down to 7 nm in diameter, which means that we had to extrapolate to 3 nm using aerosol dynamics theory. The approach used here is based on the competing processes of condensational growth and scavenging onto background aerosols, assuming time and size independent growth rate and time independent coagulation sink in the range 3 to 7 nm.

To first evaluate our extrapolation method, we applied it to particle formation events at Hyttiälä, where DMPS measurements extend down to 3 nm and formation rates at 3 nm ($J_{3,obs}$) and 7 nm ($J_{7,obs}$) can thus be determined directly from the measured size distribution evolution. The results show that the estimated daily mean values of J_3 are in reasonably good agreement with observed mean J_3 , with 84% of the estimated J_3 within a factor of two from the measured ones and, mostly overestimated. However, when considering detailed daily time evolution, the agreement is typically poor. This is caused by the fact that there is a time lag between J_3 and J_7 and to take this into account in the comparison an estimation of the growth rate *GR* is needed. Estimating GR_{3-10} , as was shown from Hyttiälä data, does not seem to give satisfactory results for this purpose. It should be noted that we have to estimate *GR* from the data above 7 nm for Puijo site due to the lack of the measured data below 7 nm.

At Puijo, the mean and median of J_7 for quantifiable particle formation days were 0.23 and $0.07 \text{ cm}^{-3} \text{ s}^{-1}$, respectively, while the extrapolated mean and median J_3 were 0.47 and $0.13 \text{ cm}^{-3} \text{ s}^{-1}$, respectively. These are about two times greater than the corresponding values in Hyttiälä. Asmi et al. (2011) reported monthly mean 7-nm particle formation rate between 0.1 and $0.2 \text{ #cm}^{-3} \text{ s}^{-1}$ for the NPF events in the sub-Arctic Pallas station, Finland. The ultimate aim of this work is to predict nucleation rates from size distribution measurements that do not extend to sizes lower than 7nm. The results obtained in this study suggest this is very challenging, in large part due to the difficulty in reliably predicting the growth rate down to around 1.5nm. It is noted that the possible size dependence of this growth rate further complicates the matter.



Acknowledgments:

280 We gratefully acknowledge the financial support by the Academy of Finland Center of Excellence program (project numbers 272041, 1118615), the Nordic Centre of Excellence CRAICC, University of Eastern Finland (UEF) strategic funding, and ACTRIS (under the European Union Seventh Framework Programme (FP7/2007–2013) grant agreement no. 262254 and Horizon 2020 research and innovation programme under grant agreement no. 654109).

References

- 285 Aalto, P., Hämeri, K., Becker, E., Weber, R., Salm, J., Mäkelä, J., Hoell, C., O'dowd, C., Hansson, H.-C., Väkevä, M., Koponen, I., Buzorius, G., and Kulmala, M.: Physical characterization of aerosol particles during nucleation events, *Tellus B* [Online], Volume 53, 2001.
- Asmi, E., Kivekäs, N., Kerminen, V.-M., Komppula, M., Hyvärinen, A.-P., Hatakka, J., Viisanen, Y., and Lihavainen, H.:
 290 Secondary new particle formation in Northern Finland Pallas site between the years 2000 and 2010, *Atmos. Chem. Phys.*, 11, 12959-12972, doi:10.5194/acp-11-12959-2011, 2011.
- Almeida, J., Schobesberger, S., Kürten, A., Ortega, I. K., Kupiainen-Määttä, O., Praplan, A. P., Adamov, A., Amorim, A., Bianchi, F., Breitenlechner, M., David, A., Dommen, J., Donahue, N. M., Downard, A., Dunne, E., Duplissy, J., Ehrhart, S., Flagan, R. C., Franchin, A., Guida, R., Hakala, J., Hansel, A., Heinritzi, M., Henschel, H., Jokinen, T., Junninen, H., Kajos,
 295 M., Kangasluoma, J., Keskinen, H., Kupc, A., Kurtén, T., Kvashin, A. N., Laaksonen, A., Lehtipalo, K., Leiminger, M., Leppä, J., Loukonen, V., Makhmutov, V., Mathot, S., McGrath, M. J., Nieminen, T., Olenius, T., Onnela, A., Petäjä, T., Riccobono, F., Riipinen, I., Rissanen, M., Rondo, L., Ruuskanen, T., Santos, F. D., Sarnela, N., Schallhart, S., Schnitzhofer, R., Seinfeld, J. H., Simon, M., Sipilä, M., Stozhkov, Y., Stratmann, F., Tomé, A., Tröstl, J., Tsagkogeorgas, G., Vaattovaara, P., Viisanen, Y., Virtanen, A., Vrtala, A., Wagner, P. E., Weingartner, E., Wex, H., Williamson, C., Wimmer, D., Ye, P.,
 300 Yli-Juuti, T., Carslaw, K. S., Kulmala, M., Curtius, J., Baltensperger, U., Worsnop, D. R., Vehkamäki, H., and Kirkby, J.: Molecular understanding of sulphuric acid-amine particle nucleation in the atmosphere. *Nature*, 502: 359-363, doi:10.1038/nature12663, 2013.
- Berndt, T., Sipilä, M., Stratmann, F., Petäjä, T., Vanhanen, J., Mikkilä, J., Patokoski, J., Taipale, R., Mauldin III, R. L., and Kulmala, M.: Enhancement of atmospheric H₂SO₄ / H₂O nucleation: organic oxidation products versus amines, *Atmos.*
 305 *Chem. Phys.*, 14, 751-764, doi:10.5194/acp-14-751-2014, 2014.
- Dal Maso, M., Kulmala, M., Riipinen, I., Wagner, R., Hussein, T., Aalto, P. P. & Lehtinen K. E. J.: Formation and growth of fresh atmospheric aerosols: eight years of aerosol size distribution data from SMEAR II, Hyytiälä, Finland, *Boreal Environment Research*. 10, 5, p. 323-336. 14 p, 2005.
- Fuzzi, S., Baltensperger, U., Carslaw, K., Decesari, S., Denier van der Gon, H., Facchini, M. C., Fowler, D., Koren, I.,
 310 Langford, B., Lohmann, U., Nemitz, E., Pandis, S., Riipinen, I., Rudich, Y., Schaap, M., Slowik, J. G., Spracklen, D. V.,



- Vignati, E., Wild, M., Williams, M., and Gilardoni, S.: Particulate matter, air quality and climate: lessons learned and future needs, *Atmos. Chem. Phys.*, 15, 8217-8299, doi:10.5194/acp-15-8217-2015, 2015.
- Hussein, T., Dal Maso, M., Petäjä, T., Koponen, I. K., Paatero, P., Aalto, P. P., Hämeri, K. & Kulmala, M.: Evaluation of an automatic algorithm for fitting the particle number size distributions. *Boreal Env. Res.* 10: 337–355, 2005.
- 315 Iida, K., Stolzenburg, M. R., McMurry, P. H.: Effect of Working Fluid on Sub-2 nm Particle Detection with a Laminar Flow Ultrafine Condensation Particle Counter, *Aerosol Science and Technology*, 43:1, 81-96, doi: 10.1080/02786820802488194, 2009.
- Jokinen, V. and Mäkelä, J. M.: Closed-loop arrangement with critical orifice for DMA sheath/excess flow system, *J. Aerosol Sci.*, 28, 643–648, 1997.
- 320
- Kerminen, V.-M., & Kulmala, M.: Analytical formulae connecting the “real” and the “apparent” 25 nucleation rate and the nuclei number concentration for atmospheric nucleation events. *Journal of Aerosol Science*, 33, 609–622, doi: [http://dx.doi.org/10.1016/S0021-8502\(01\)00194-X](http://dx.doi.org/10.1016/S0021-8502(01)00194-X), 2002.
- Kerminen, V.-M., Lehtinen, K. E. J., Anttila, T. and Kulmala, M.: Dynamics of atmospheric nucleation mode particles: a
- 325 timescale analysis. *Tellus B*, 56, 135-146, doi: 10.1111/j.1600-0889.2004.00095.x, 2003.
- Kerminen, V.-M., Anttila, T., Lehtinen, K. E. J. and Kulmala, M.: Parameterization for atmospheric new-particle formation: Application to a system involving sulfuric acid and condensable water-soluble organic vapors, *Aerosol Sci. Tech.* 38, 1001-1008, doi: 10.1080/027868290519085, 2004.
- Kerminen, V.-M., Paramonov, M., Anttila, T., Riipinen, I., Fountoukis, C., Korhonen, H., Asmi, E., Laakso, L.,
- 330 Lihavainen, H., Swietlicki, E., Svenningsson, B., Asmi, A., Pandis, S. N., Kulmala, M., and Petäjä, T.: Cloud condensation nuclei production associated with atmospheric nucleation: a synthesis based on existing literature and new results, *Atmos. Chem. Phys.*, 12, 12037-12059, doi:10.5194/acp-12-12037-2012, 2012.
- Kirkby, J., Duplissy, J., Sengupta, K., Frege, C., Gordon, H., Williamson, C., Heinritzi, M., Simon, M., Yan, C., Almeida, J., Tröstl, J., Nieminen, T., Ortega, I. K., Wagner, R., Adamov, A., Amorim, A., Bernhammer, A.-K., Bianchi, F.,
- 335 Breitenlechner, M., Brilke, S., Chen, X., Craven, J., Dias, A., Ehrhart, S., Flagan, R. C., Franchin, A., Fuchs, C., Guida, R., Hakala, J., Hoyle, C. R., Jokinen, T., Junninen, H., Kangasluoma, J., Kim, J., Krapf, M., Kürten, A., Laaksonen, A., Lehtipalo, K., Makhmutov, V., Mathot, S., Molteni, U., Onnela, A., Peräkylä, O., Piel, F., Petäjä, T., Praplan, A. P., Pringle, K., Rap, A., Richards, N. A. D., Riipinen, I., Rissanen, M. P., Rondo, L., Sarnela, N., Schobesberger, S., Scott, C. E., Seinfeld, J. H., Sipilä, M., Steiner, G., Stozhkov, Y., Stratmann, F., Tomé, A., Virtanen, A., Vogel, A. L., Wagner, A.,
- 340 Wagner, P. E., Weingartner, E., Wimmer, D., Winkler, P. M., Ye, P., Zhang, X., Hansel, A., Dommen, J., Donahue, N. M., Worsnop, D. R., Baltensperger, U., Kulmala, M., Carslaw, K. S., Curtius, J.: Ion-induced nucleation of pure biogenic particles, *Nature*, doi:10.1038/nature12663, 2016.



- 345 Korhonen, P., Kulmala, M., Laaksonen, A., Viisanen, Y., McGraw, R. and Seinfeld, J. H.: Ternary nucleation of H₂SO₄, NH₃, and H₂O in the atmosphere, *Journal of Geophysical Research: Atmospheres*, 104, 26349–26353, doi = 10.1029/1999JD900784, 1999.
- Korhonen, H., Kerminen, V. M., Kokkola, H., and Lehtinen, K. E. J.: Estimating atmospheric nucleation rates from size distribution measurements: Analytical equations for the case of size dependent growth rates, *Journal of Aerosol Science*, 69, 13-20, doi:http://dx.doi.org/10.1016/j.jaerosci.2013.11.006, 2014.
- 350 Kuang, C., Chen, M., McMurry, P. H., and Wang, J.: Modification of laminar flow ultrafine condensation particle counters for the enhanced detection of 1 nm condensation nuclei, *Aerosol Sci. Technol.*, 46, 309–315, 2012.
- Kürten, A., Williamson, C., Almeida, J., Kirkby, J., and Curtius, J.: On the derivation of particle nucleation rates from experimental formation rates, *Atmos. Chem. Phys.*, 15, 4063-4075, doi:10.5194/acp-15-4063-2015, 2015.
- Kulmala, M., Liisa, P., and Mäkelä, J. M.: Stable sulphate clusters as a source of new atmospheric particles, *Nature* 404, no. 6773, 66-69, doi: 10.1038/35003550, 2000.
- 355 Kulmala M., Hämeri K., Aalto P. P., Mäkelä J. M., Pirjola L., Nilsson E. D., Buzorius G., Rannik Ü., Maso M. D., Seidl W., Hoffman T., Janson R., Hansson H.-C., Viisanen Y., Laaksonen A. & O'Dowd C. D.: Overview of the international project on biogenic aerosol formation in the boreal forest (BIOFOR). *Tellus B*, 53: 324–343. doi: 10.1034/j.1600-0889.2001.530402, 2001.
- 360 Kulmala, M., Vehkamäki, H., Petäjä, T., Dal Maso, M., Lauri, A., Kerminen, V.-M., Birmili, and W., McMurry, P.H.: Formation and growth rates of ultrafine atmospheric particles: a review of observations, *J Aerosol Sci.*, 35:143-76, doi:10.1016/j.jaerosci.2003.10.003, 2004.
- Kulmala, M., Lehtinen, K. E. J., and Laaksonen, A.: Cluster activation theory as an explanation of the linear dependence between formation rate of 3 nm particles and sulphuric acid concentration, *Atmos. Chem. Phys.*, 6, 787–793, doi:10.5194/acp-6-787-2006, 2006.
- 365 Kulmala, M., Petäjä, T., Nieminen, T., Sipilä, M., Manninen, H. E, Lehtipalo, K., Dal Maso, M., Aalto, P. P, Junninen, H., Paasonen, P., Riipinen, I., Lehtinen, K. E J, Laaksonen, A., Kerminen, V.-M.: Measurement of the nucleation of atmospheric aerosol particles, 7, 1651–1667, doi: http://dx.doi.org/10.1038/nprot.2012.091, 2012.
- 370 Kulmala, M., Kontkanen, J., Junninen, H., Lehtipalo, K., Manninen, H. E., Nieminen, T., Petäjä, T., Sipilä, M., Schobesberger, S., Rantala, P., Franchin, A., Jokinen, T., Järvinen, E., Äijälä, M., Kangasluoma, J., Hakala, J., Aalto, P. P., Paasonen, P., Mikkilä, J., Vanhanen, J., Aalto, J., Hakola, H., Makkonen, U., Ruuskanen, T., Mauldin, R. L., Duplissy, J., Vehkamäki, H., Bäck, J., Kortelainen, A., Riipinen, I., Kurten, T., Johnston, M. V., Smith, J. N., Ehn, M., Mentel, T. F., Lehtinen, K. E. J., Laaksonen, A., Kerminen, V.-M., Worsnop, D. R.: Direct Observations of Atmospheric Aerosol Nucleation, 339, 943–946, doi: 10.1126/science.1227385, 2013.
- 375 Laakso, L., Petäjä, T., Lehtinen, K. E. J., Kulmala, M., Paatero, J., Hörrak, U., Tammet, H., and Joutsensaari, J.: Ion production rate in a boreal forest based on ion, particle and radiation measurements, *Atmos. Chem. Phys.*, 4, 1933-1943, doi:10.5194/acp-4-1933-2004, 2004.



- Laaksonen, A., Kulmala, M., Berndt, T., Stratmann, F., Mikkonen, S., Ruuskanen, A., Lehtinen, K. E. J., Dal Maso, M., Aalto, P., Petäjä, T., Riipinen, I., Sihto, S.-L., Janson, R., Arnold, F., Hanke, M., Ücker, J., Umann, B., Sellegri, K., O'Dowd, C. D., and Viisanen, Y.: SO₂ oxidation products other than H₂SO₄ as a trigger of new particle formation. Part 2: Comparison of ambient and laboratory measurements, and atmospheric implications, *Atmos. Chem. Phys.*, 8, 7255-7264, doi:10.5194/acp-8-7255-2008, 2008.
- Lehtinen, K. E. J., dal Maso, M., Kulmala, M., and Kerminen, V.-M.: Estimating nucleation rates from apparent particle formation rates and vice versa: Revised formulation of the Kerminen–Kulmala equation, *J. Aerosol Sci.*, 38, 988–994, 2007.
- Leskinen, A., Portin, H., Komppula, M., Miettinen, P., Arola, A., Lihavainen, H., Hatakka, J., Laaksonen, A., Lehtinen, K. E. J.: Overview of the research activities and results at Puijo semiurban measurement station, *Boreal Env. Res.*, 14, 576–590, 2009.
- McMurry, P. H., and S. K. Friedlander: New particle formation in the presence of an aerosol, *Atmos. Environ.*, 13, 1635 – 1651, 1979.
- McMurry, P. H., & Wilson, J. C.: Growth laws for the formation of secondary ambient aerosols: Implications for chemical conversion mechanisms. *Atmospheric Environment* (1967), 16(1), 121-134. doi:10.1016/0004-6981(82)90319-5, 1982.
- McMurry, P. H.: New particle formation in the presence of an aerosol: Rates, time scales and sub-0.01 μm size distributions, *J. Colloid Interface Sci.*, 95(1), 72 – 80, 1983.
- Merikanto, J., Spracklen, D. V., Mann, G. W., Pickering, S. J., and Carslaw, K. S.: Impact of nucleation on global CCN, *Atmos. Chem. Phys.*, 9, 8601-8616, doi:10.5194/acp-9-8601-2009, 2009.
- Minguillón, M. C., Brines, M., Pérez, N., Reche, C., Pandolfi, M., Fonseca, A. S., Amato, F., Alastuey, A., Lyasota, A., Codina, B., Lee, H.-K., Eun, H.-R., Ahn, K.-H., Querol, X.: New particle formation at ground level and in the vertical column over the Barcelona area, *Atmospheric Research*, Volumes 164–165, Pages 118-130, doi:10.1016/j.atmosres.2015.05.003, 2015.
- Nie, W., Ding, A., Wang, T., Kerminen, V.-M., George, C., Xue, L., Wang, W., Zhang, Q., Petäjä, T., Qi, X., Gao, X., Wang, X., Yang, X., Fu, C., Kulmala, M.: Polluted dust promotes new particle formation and growth, *Atmos. Chem. Phys.*, 4, 6634, doi:10.1038/srep06634, 2014.
- Portin, H., Leskinen, A., Hao, L., Kortelainen, A., Miettinen, P., Jaatinen, A., Laaksonen, A., Lehtinen, K. E. J., Romakkaniemi, S., and Komppula, M.: The effect of local sources on particle size and chemical composition and their role in aerosol–cloud interactions at Puijo measurement station, *Atmos. Chem. Phys.*, 14, 6021-6034, doi:10.5194/acp-14-6021-2014, 2014.
- Sgro, L. A., Fernández de la Mora, J.: A Simple Turbulent Mixing CNC for Charged Particle Detection Down to 1.2 nm, *IEEE Trans. Aerosp. Electron. Syst.*, 38, 1-11, 10.1080/02786820490247560, 2004.
- Vanhanen, J., Mikkilä, J., Lehtipalo, K., Sipilä, M., Manninen, H. E., Siivola, E., Petäjä, T., Kulmala, M.: Particle Size Magnifier for Nano-CN Detection, *Aerosol Science and Technology*, 45:4, 533-542, 2011.



- 410 Vuollekoski, H., Sihto, S.-L., Kerminen, V.-M., Kulmala, M., and Lehtinen, K. E. J.: A numerical comparison of different methods for determining the particle formation rate, *Atmos. Chem. Phys.*, 12, 2289-2295, doi:10.5194/acp-12-2289-2012, 2012.
- Weber, R. J., McMurry, P. H., Eisele, F. L., Tanner, D. J.: Measurement of Expected Nucleation Precursor Species and 3–500-nm Diameter Particles at Mauna Loa Observatory, Hawaii, *Journal of the Atmospheric Sciences* 1995 52:12, 2242-415 2257, 1995.
- 415 Weber, R. J., Marti, J. J., and McMurry, P. H., Eisele, F. L., Tanner, D. J., and Jefferson, A.: Measured atmospheric new particle formation rates: implications for nucleation mechanisms, *Chemical Engineering Communications*, 151, 53-64, doi: 10.1080/00986449608936541, 1996.
- Wimmer, D., Lehtipalo, K., Franchin, A., Kangasluoma, J., Kreissl, F., Kürten, A., Kupc, A., Metzger, A., Mikkilä, J., 420 Petäjä, T., Riccobono, F., Vanhanen, J., Kulmala, M., and Curtius, J.: Performance of diethylene glycol-based particle counters in the sub-3 nm size range, *Atmos. Meas. Tech.*, 6, 1793–1804, doi:10.5194/amt-6-1793-2013, 2013.
- Winklmayr, W., Reischl, G. P., Linder, A. O., and Berner, A.: A new electromobility spectrometer for the measurement of aerosol size distribution in the size range 1 to 1000 nm, *J. Aerosol Sci.*, 22, 289–296, 1991.
- Yli-Juuti, T., Nieminen, T., Hirsikko, A., Aalto, P. P., Asmi, E., Hörrak, U., Manninen, H. E., Patokoski, J., Dal Maso, M., 425 Petäjä, T., Rinne, J., Kulmala, M., and Riipinen, I.: Growth rates of nucleation mode particles in Hyytiälä during 2003–2009: variation with particle size, season, data analysis method and ambient conditions, *Atmos. Chem. Phys.*, 11, 12865-12886, doi:10.5194/acp-11-12865-2011, 2011.
- Xiao, S., Wang, M. Y., Yao, L., Kulmala, M., Zhou, B., Yang, X., Chen, J. M., Wang, D. F., Fu, Q. Y., Worsnop, D. R., and Wang, L.: Strong atmospheric new particle formation in winter in urban Shanghai, China, *Atmos. Chem. Phys.*, 15, 1769-430 1781, doi:10.5194/acp-15-1769-2015, 2015.
- Zhou, J.: Hygroscopic Properties of Atmospheric Aerosol Particles in Various Environments, PhD thesis, University of Lund, Division of Nuclear Physics, Sweden, <http://lup.lub.lu.se/record/41435>, 2001.



435

Table 1: Seasonal means of observed formation rate of 7-nm particles ($J_{7,obs}$), estimated formation rate of 3-nm particles ($J_{3,est}$), growth rate of particles in nucleation mode size range 7-20 nm (GR_{7-20}) and coagulation sink of nucleation mode particles onto larger particles ($CoagS(d=7\text{ nm})$) for NPF days which occurred at Puijo during Apr 2007 - Dec 2015. Note that because there is only one NPF event which occurred in winter, we excluded winter from the table.

	$J_{7,obs}$ (#cm ⁻³ s ⁻¹)	$J_{3,est}$ (#cm ⁻³ s ⁻¹)	GR_{7-20} (nm/h)	$CoagS(d=7\text{ nm})$ (1/s)
Spring (Mar-May)	0,53	0,24	2,30	1.8×10^{-4}
Summer (Jun-Aug)	0,52	0,30	4,14	2.3×10^{-4}
Fall (Sep-Nov)	0,22	0,12	3,01	1.5×10^{-4}
Overall	0.23	0.47	2.70	1.9×10^{-4}

440

445



450 Figure and figure captions

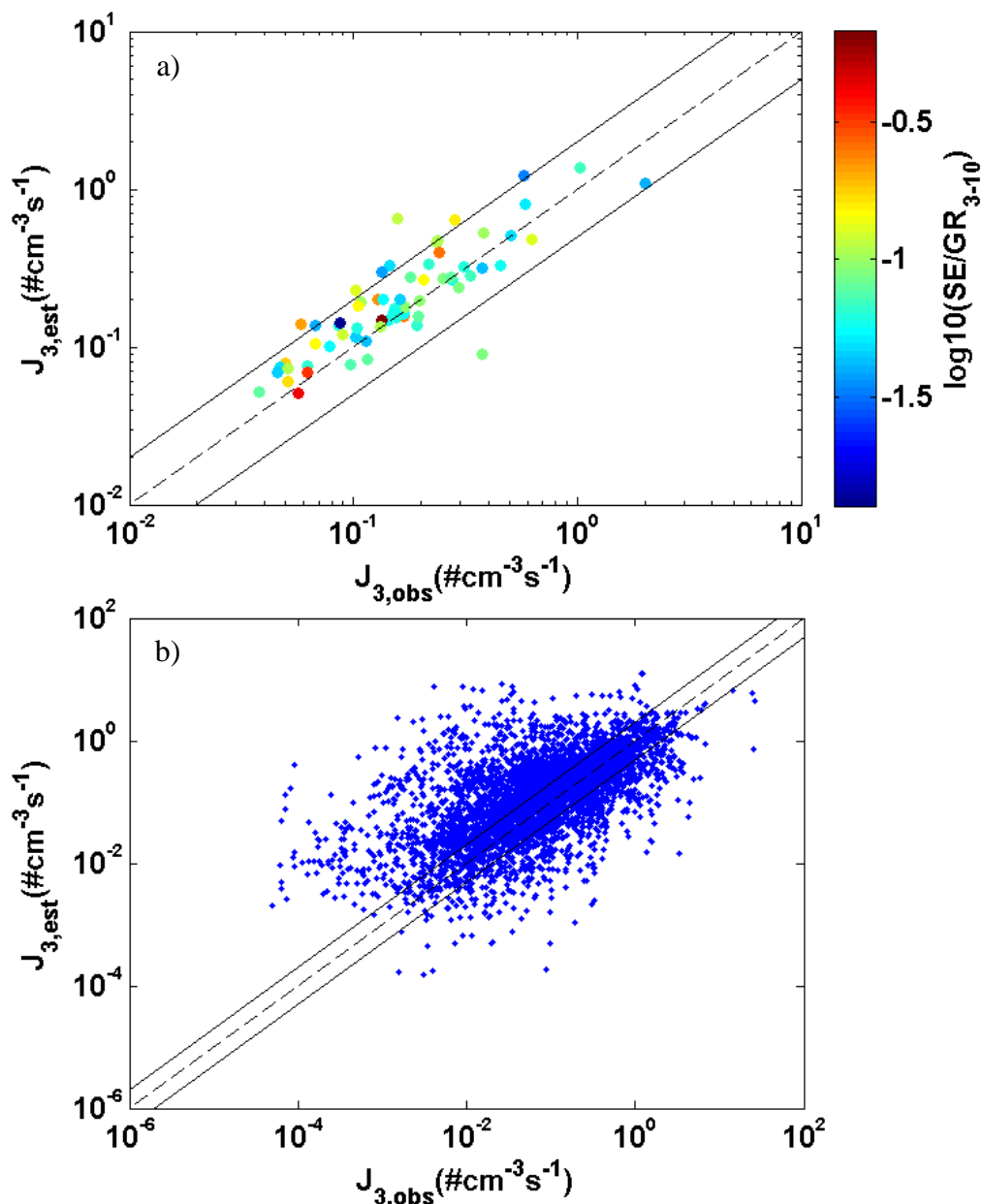
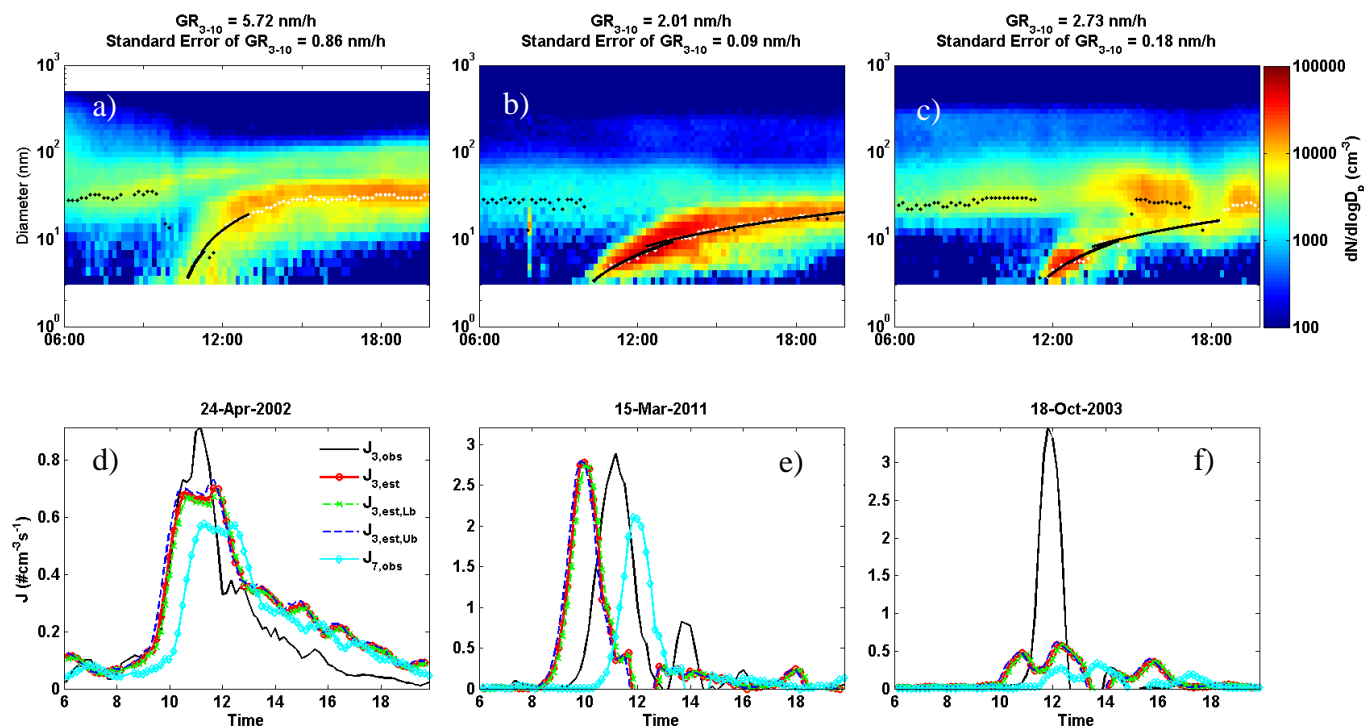


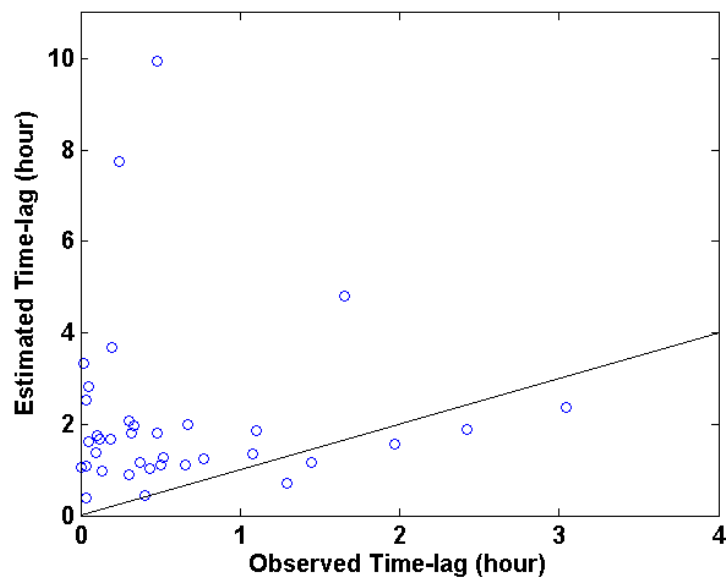
Figure 1: Estimated ($J_{3,est}$) against observed ($J_{3,obs}$) formation rates of 3 nm particles ($\text{\#cm}^{-3}\text{s}^{-1}$) during new-particle formation (NPF) event days in Hyytiälä. Data points indicate a) 10-minute b) arithmetic mean J_3 between 07:00 to 19:00 local time for each NPF day. The color code indicates the ratio of standard error (SE) of GR_{3-10} estimates through linear fitting and GR_{3-10} itself.



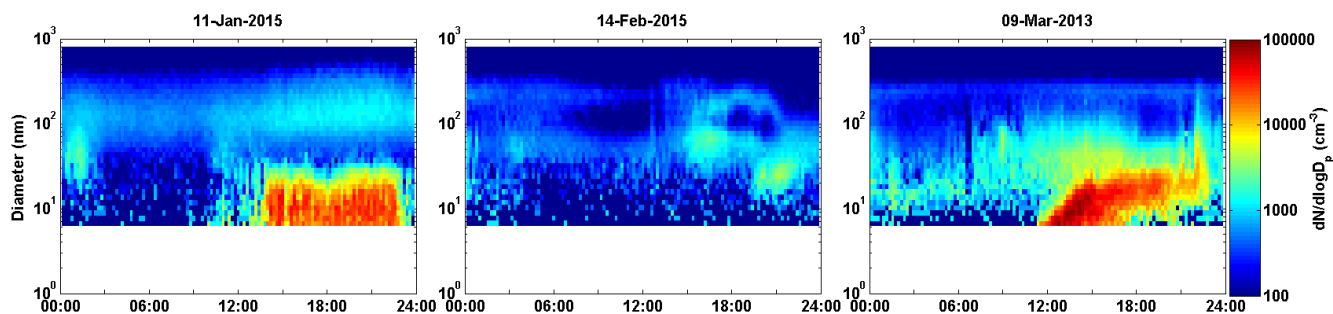
455 The aerosol size distribution temporal resolution measured by DMPS at Hyttiälä is 10-minute. Note that the time-lag during which 3 nm particles grow to 7 nm particles is taken into account in the $J_{3,est}$.



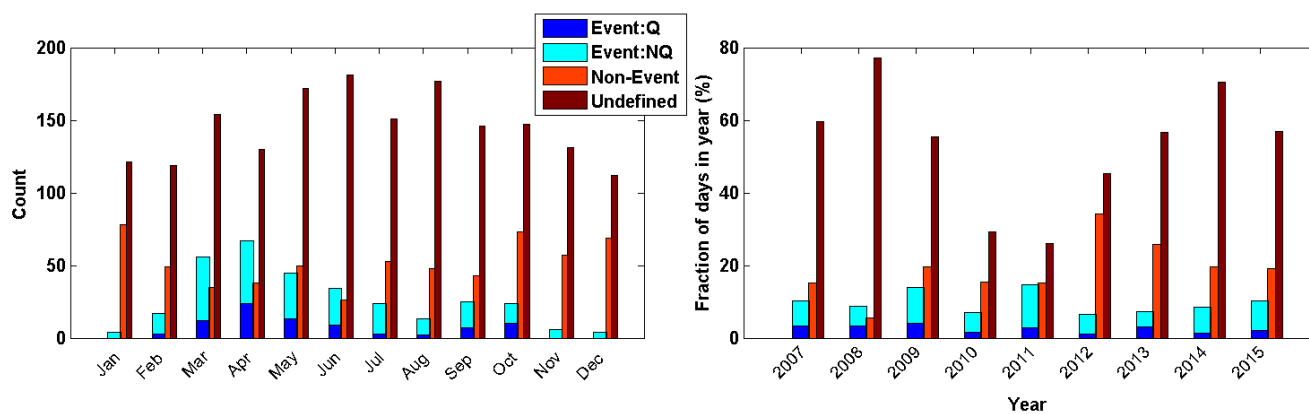
460 Figure 2: Examples of Hyttiälä NPF events. a, b, and c) the evolution of the particle size distribution. White dots
 represent the geometric mean diameter of the nucleation mode determined by log-normal fitting, and the solid black
 line shows the first-order polynomial fit. Figures d), e) and f) are the corresponding evolution of 3 nm particle
 formation rates obtained from Eq. (2) (red), observed $J_{3,obs}$ (black) and observed formation rates of 7 nm particles
 $J_{7,obs}$ (cyan). The dashed curves show the upper bound ($J_{3,est,Ub}$) and lower bound ($J_{3,est,Lb}$) calculated using Eq. (2)
 465 inputting the lower ($GR_{3-10} - SE$) and upper ($GR_{3-10} + SE$) bound of GR_{3-10} , respectively.



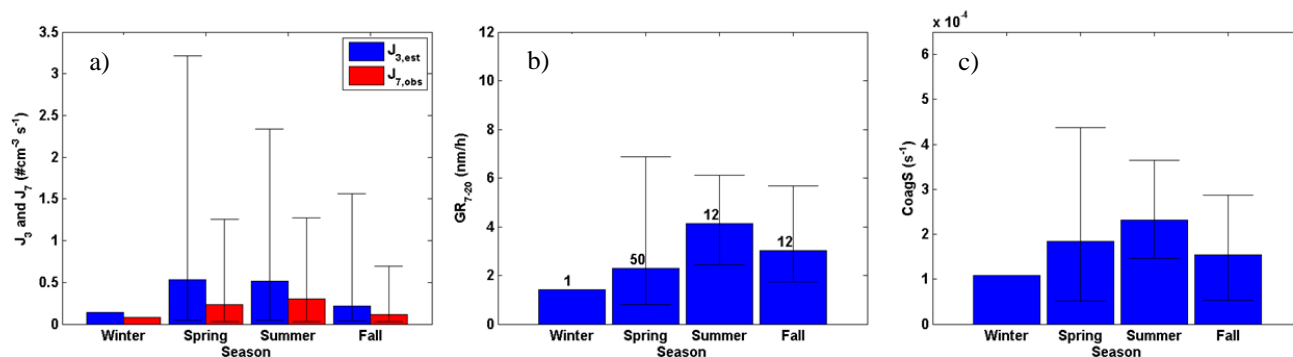
470 **Figure 3:** Time lag between formation of 3 nm and 7 nm particles for NPF days at Hyytiälä determined visually from the time difference between the $J_{7,obs}$ and $J_{3,obs}$ peak (x-axis) and $t' - t = 4 \text{ nm}/GR_{3-10}$ (y-axis) which is also equal to the time difference between $J_{7,obs}$ and $J_{3,est}$.



475 **Figure 4:** Examples of the time evolution of the aerosol size distribution in Puijo for (a) an undefined day characterized by a burst in the number concentrations of the small particles which doesn't have the characteristics of a typical NPF event day (b) a typical undefined day, and (c) a clear NPF event day.



480 **Figure 5:** Monthly number (left panel) and yearly fraction (right panel) of NPF event days (divided into Quantifiable Events (Q) and Non-Quantifiable events (NQ)), Non-Events (NE) and undefined days recorded in Puijo during period 2007-2015. Fraction of (e.g. NE) days in year is the ratio of number of NEs and number of days within the year. Note that the days for which bad or no data were recorded are not shown here. Note that 48 and 44% of the days are missing during years 2010 and 2012, respectively.



485 **Figure 6.** Seasonal mean values of different parameters for NPF days at Puijo: a) estimated formation rates of 3-nm particles ($J_{3,est}$) and observed formation rates of 7-nm particles ($J_{7,obs}$) b) growth rate of the particles within size range 7-20 nm c) coagulation sink ($CoagS$) of 7-nm particles. The height of the bars shows the mean values of data points (i.e. mean values during 7:00 to 19:00 of the J and $CoagS$ values for 75 NPF event days) within each season, and the error bars indicate the values between minimum and maximum of the data points. The numbers on top of each bar in middle panel indicate the number of the NPF events in corresponding season. The same applies to the figure 6-a and 6-c.

490